Inorg. Chem. **2002**, *41*, 2151–2157

A Hybrid Consisting of Coordination Polymer and Noncovalent Organic Networks: A Highly Ordered 2-D Phenol Network Assembled by Edge-to-Face π–π Interactions

Jung Woo Ko, Kil Sik Min, and Myunghyun Paik Suh*

School of Chemistry and Molecular Engineering, Center for Molecular Catalysis, Seoul National University, Seoul 151-747, Republic of Korea

Received December 14, 2001

A 2-D metal–organic open framework having 1-D channels, $[Cu(C_{10}H_{26}N_6)]_3[C_6H_3(COO)_3]_2 \cdot 18H_2O$ (**1**), was constructed by the self-assembly of the Cu(II) complex of hexaazamacrocycle **A** (**A** = $C_{10}H_{26}N_6$) with sodium 1,3,5-benzenetricarboxylate (BTC^{3-}) in DMSO–H_2O solution. **1** crystallizes in the trigonal space group $P\bar{3}$ with $a = b = 17.705(1)$ Å, $c = 6.940(1)$ Å, $\alpha = \beta = 90^\circ$, $\gamma = 120^\circ$, $V = 1884.0(3)$ Å^3, $Z = 1$, and $\rho_{calcd} = 1.428$ g cm^{-3}. The X-ray crystal structure of **1** indicates that each Cu(II) macrocyclic unit binds two BTC^{3-} ions in a trans position and each BTC^{3-} ion coordinates three Cu(II) macrocyclic complexes to form 2-D coordination polymer layers with honeycomb cavities (effective size 8.1 Å), and the layers are packed to generate 1-D channels perpendicularly to the 2-D layers. Solid **1** binds guest molecules such as MeOH, EtOH, and PhOH with different binding constant and capacity. By the treatment of **1** with aqueous solution of phenol, a hybrid solid $[Cu(C_{10}H_{26}N_6)]_3[C_6H_3(COO)_3]_2 \cdot 9PhOH \cdot 6H_2O$ (**2**) was assembled. **2** crystallizes in the trigonal $R3$ space group with $a = b = 20.461(1)$ Å, $c = 24.159(1)$ Å, $\alpha = \beta = 90^\circ$, $\gamma = 120^\circ$, $V = 8759.2(7)$ Å^3, $Z = 3$, and $\rho_{calcd} = 1.280$ g cm^{-3}. In **2**, highly ordered 2-D noncovalent phenol layers are formed by the edge-to-face π–π interactions between the phenol molecules and are alternately packed with the coordination polymer layers in the crystal lattice.

Introduction

Crystal engineering has provided a useful paradigm for the design of metal−organic polymers with tunable properties by the choice of building blocks. In particular, metal−organic open frameworks can be designed and constructed to generate cavities or channels of various sizes and shapes. Such modular open frameworks might find applications to molecular adsorption and separation processes,[1−3] ion exchange,[4,5] catalysis,[6,7] sensor technology,[8,9] optoelectronics,[10] and casting for nanowires.[11]

For the design and assembly of metal−organic open frameworks, a macrocyclic complexes can be employed as useful metal building blocks since they provide fixed numbers of vacant coordination sites at the fixed positions, which enables the extending direction of the network to be controllable.[12−15] In addition, slight change in the macrocyclic structure alters solvent binding ability of the metal ion,[16,17] which results in the different topology of the self-assembled networks.[3,18] For example, in the self-assembly of nickel(II)

* To whom correspondence should be addressed. Fax: (+82)2 8868516. E-mail: mpsuh@snu.ac.kr.

(1) (a) Li, H.; Eddaoudi, M.; O'Keeffe, M.; Yaghi, O. M. *Nature* **1999**, *402*, 276. (b) Chui, S. S.-Y.; Lo, S. M.-F.; Charmant, J. P. H.; Orpen, A. G.; Williams, I. D. *Science* **1999**, *283*, 1148.
(2) (a) Noro, S.-I.; Kitagawa, S.; Kondo, M.; Seki, K. *Angew. Chem., Int. Ed. Engl.* **2000**, *39*, 2082. (b) Kondo, M.; Yoshitomi, T.; Seki, K.; Matsuzaka, H.; Kitagawa, S. *Angew. Chem., Int. Ed. Engl.* **1997**, *36*, 1725.
(3) (a) Choi, H. J.; Lee, T. S.; Suh, M. P. *Angew. Chem.* **1999**, *111*, 1490. (b) *Angew. Chem., Int. Ed. Engl.* **1999**, *38*, 1405.
(4) Min, K. S.; Suh, M. P. *J. Am. Chem. Soc.* **2000**, *122*, 6834.
(5) Yaghi, O. M.; Li, H. *J. Am. Chem. Soc.* **1996**, *118*, 295.
(6) Seo, J. S.; Whang, D.; Lee, H.; Jun, S. I.; Oh, J.; Jeon, Y. J.; Kim, K. *Nature* **2000**, *404*, 982.
(7) Sawaki, T.; Aoyama, Y. *J. Am. Chem. Soc.* **1999**, *121*, 4793.
(8) Albrecht, M.; Lutz, M.; Spek, A. L.; van Koten, G. *Nature* **2000**, *406*, 970.
(9) Real, J. A.; Andrés, E.; Muñoz, M. C.; Julve, M.; Granier, T.; Bousseksou, A.; Varret, F. *Science* **1995**, *268*, 265.
(10) Evans, O. R.; Lin, W. *Chem. Mater.* **2001**, *13*, 2705.
(11) Hong, B. H.; Bae, S. C.; Lee, C.-W.; Jeong, S.; Kim, K. S. *Science* **2001**, *294*, 348.
(12) Choi, H. J.; Suh, M. P. *J. Am. Chem. Soc.* **1998**, *120*, 10622.
(13) Choi, H. J.; Suh, M. P. *Inorg. Chem.* **1999**, *38*, 6309.
(14) Min, K. S.; Suh, M. P. *Chem. Eur. J.* **2001**, *7*, 303.
(15) Min, K. S.; Suh, M. P. *Eur. J. Inorg. Chem.* **2001**, 449.
(16) Suh, M. P.; Kang, S.-G. *Inorg. Chem.* **1988**, *27*, 2544.
(17) Suh, M. P. *Adv. Inorg. Chem.* **1997**, 44, 93.

10.1021/ic011281u CCC: $22.00
Published on Web 03/28/2002

cyclam complex (cyclam = $C_{10}H_{24}N_4$) with 1,3,5-benzenetricarboxylate (BTC^{3-}) in water, the nickel(II) complex binds water at the axial sites and the coordinated water molecules form hydrogen bonds with BTC^{3-} to form a 3-D network which generates 1-D channels perpendicularly to the 2-D layers.[3] In this framework, positively charged inorganic and negatively charged organic layers are alternately packed. On the other hand, in the self-assembly of Ni(II) complex of similar macrocyclic ligand $C_{10}H_{26}N_6$ (**A**) with BTC^{3-}, the nickel complex directly coordinates BTC^{3-} ligand to generate the 2-D network of brick-wall motifs generating 1-D channels that are tilted with respect to the 2-D layers.[18] We expected that change of the metal ion would also affect the supramolecular structure and thus tried the Cu(II) complex in this study. Furthermore, Cu(II) macrocyclic complexes are the unexplored class of building blocks because of their weak binding property at the axial sites, due to the Jahn−Teller effect.

Hybrid solids are of great interest because of the possibility to obtain novel molecular materials having two components that are difficult or impossible to combine in a conventional solid.[19−21] We have been interested in developing synthetic strategies for the construction of hybrid materials on the basis of crystal engineering and the host−guest concept. In particular, we tried to combine coordination polymer layers and organic networks in a crystal lattice because it might provide the method for aligning the organic molecules to generate specific properties.

Here we report a new 2-D metal−organic open framework, $[Cu(C_{10}H_{26}N_6)]_3[C_6H_3(COO)_3]_2\cdot 18H_2O$ (**1**), which is self-assembled from Cu(II) hexaazamacrocyclic complex $[Cu(\mathbf{A})]^{2+}$ and Na_3BTC in DMSO−water, and its hybrid solid with highly ordered noncovalent 2-D phenol network, $[Cu(C_{10}H_{26}N_6)]_3[C_6H_3(COO)_3]_2\cdot 9PhOH\cdot 6H_2O$ (**2**).

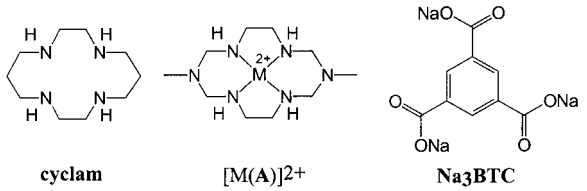

Experimental Section

General Methods. All chemicals and solvents used in the syntheses were of reagent grade and used without further purification. $[Cu(\mathbf{A})](ClO_4)_2$ was prepared according to the literature methods reported previously.[16] Infrared spectra were recorded with a Perkin-Elmer 2000 FT-IR spectrophotometer. Elemental analyses were performed by the analytical laboratory of Seoul National University. X-ray powder diffraction (XRPD) data were recorded on a Mac Science M18XHF-22 diffractometer at 50 kV and 100 mA for Cu Kα (λ = 1.54050 Å) with a scan speed of 5°/min and a step size of 0.02° in 2θ. Thermogravimetric analysis (TGA) and differential thermal analysis (DTA) were performed under N_2(g) at a scan rate of 5 °C/min using a Rigaku Tas-100 system.

$[Cu(C_{10}H_{26}N_6)]_3[BTC]_2\cdot 18H_2O$ (1). To a DMSO solution (20 mL) of $[Cu(C_{10}H_{26}N_6)](ClO_4)_2$ (**A**)[16] (0.38 g, 0.77 mmol) was added dropwise an aqueous solution (10 mL) of Na_3BTC (0.25 g, 0.91 mmol). The solution was allowed to stand at room temperature until small purple crystals formed over several days. The crystals were filtered off, washed with MeOH, and dried in air. Long rod-shaped single crystals suitable for X-ray diffraction study were obtained by recrystallization of the product from hot water. Yield: 58%. Anal. Calcd for $Cu_3C_{48}H_{120}N_{18}O_{30}$: C, 35.58; H, 7.47; N, 15.56. Found: C, 35.54; H, 5.96; N, 15.61. FT-IR (Nujol mull, cm^{-1}): 3391 (s, br), 3252 (s), 3181 (s), 1620 (s), 1569 (s). UV/vis (diffuse reflectance spectrum, λ_{max}): 275, 514 nm.

$[Cu(C_{10}H_{26}N_6)]_3[C_6H_3(COO)_3]_2\cdot 9PhOH\cdot 6H_2O$ (2). Crystal **1** (0.29 g, 0.18 mmol) was dissolved in water (3 mL), and an aqueous solution (5 mL) of phenol (0.46 g, 4.9 mmol) was added dropwise. The solution was allowed to stand at room temperature until cubic-shaped violet crystals formed in 1−2 days, which were filtered off, washed with the aqueous solution (2.5 mL) of phenol (0.23 g), and dried in air. Yield: 87%. Anal. Calcd for $Cu_3C_{102}H_{150}N_{18}O_{27}$: C, 54.42; H, 6.72; N, 11.20. Found: C, 54.91; H, 5.46; N, 10.72. FT-IR (Nujol mull, cm^{-1}): 3267 (s), 3148 (s), 1652 (m), 1605 (s), 1559 (s), 1349 (s). UV/vis (diffuse reflectance spectrum, λ_{max}): 275, 538 nm.

X-ray Diffraction Measurements. Intensity data for **1** and **2** were collected with an Enraf-Nonius Kappa CCD diffractometer (Mo Kα, λ = 0.71073 Å, graphite monochromator). Preliminary orientation matrixes and unit cell parameters were obtained from the peaks of the first 10 frames and were then refined using the whole data set. Frames were integrated and corrected for Lorentz and polarization effects using DENZO.[22] The scaling and the global refinement of crystal parameters were performed by SCALEPACK.[22] No absorption correction was made. The crystal structures were solved by the direct methods[23] and refined by full-matrix least-squares refinement using the SHELXL93 computer program.[24] The positions of all non-hydrogen atoms were refined with anisotropic displacement factors. The hydrogen atoms were positioned geometrically and refined using a riding model. The crystallographic data for **1** and **2** are summarized in Table 1, and the selected bond distances and angles are listed in Tables 2 and 3.

Binding Study of 1 with Organic Guests. Pale purple crystals of **1** as synthesized were ground in a mortar until they became microcrystalline powder. The solid (10−32 mg) whose weight was exactly measured was immersed in the toluene solutions (2 mL) containing methanol, ethanol, and phenol, respectively, for 12 h at 25 °C. The initial concentrations of methanol, ethanol, and phenol were varied as 6.24×10^{-2}−9.30×10^{-1}, 2.60×10^{-2}−6.08×10^{-1}, and 4.25×10^{-3}−1.37 M, respectively, to keep the saturation values ranging 20−80%. The concentration change of the organic guests was measured by GC using dodecane as the internal standard.

The binding constant (K_f) between a binding site (BS) of the insoluble host and a guest molecule (G) can be defined as k_{ad}/k_{de} (eq 1) by analogy with the Langmuir isotherm for adsorption of gas molecules on solid surfaces.

(18) Choi, H. J.; Suh, M. P. *J. Inclusion Chem.* **2001**, *41*, 155.
(19) Biradha, K.; Domasevitch, K. V.; Moulton, B.; Seward, C.; Zaworotko, M. J. *Chem. Commun.* **1999**, 1327.
(20) Biradha, K.; Mondal, A.; Moulton, B.; Zaworotko, M. J. *J. Chem. Soc., Dalton Trans.* **2000**, 3837.
(21) Coronado, E.; Galan-Mascaros, J. R.; Gomez-Garcia, C. J.; Laukhin, V. *Nature* **2000**, *408*, 447.
(22) Otwinowsky, Z.; Minor, W. Processing of X-ray Diffraction Data Collected in Oscillation Mode. In *Methods in Enzymology*; Carter, C. W., Jr., Sweet, R. M., Eds.; Academic Press: New York, 1996; Vol. 276, p 307.
(23) Sheldrick, G. M. *Acta Crystallogr*. **1990**, *A46*, 467.
(24) Sheldrick, G. M. *SHELXL93. Program for the crystal structure refinement*; University of Göttingen: Göttingen, Germany, 1993.

Table 1. Crystallographic Data for **1** and **2**

	1	**2**
empirical formula	$Cu_3C_{48}H_{120}N_{18}O_{30}$	$Cu_3C_{102}H_{150}N_{18}O_{27}$
fw	1620.24	2251.02
space group	$P\bar{3}$, trigonal	$R3$, trigonal
a, Å	17.705(1)	20.461(1)
b, Å	17.705(1)	20.461(1)
c, Å	6.940(1)	24.159(1)
α, deg	90	90
β, deg	90	90
γ, deg	120	120
V, Å^3	1884.0(3)	8759.2(7)
Z	1	3
ρ_{calc}, g cm^{-3}	1.428	1.280
T, °C	20(2)	20(2)
μ, mm^{-1}	0.929	0.618
R_1 (4σ data)[a]	0.1062	0.0742
wR_2 (4σ data)[b]	0.2605	0.1816

[a] $R_1 = \Sigma||F_o| - |F_c||/\Sigma|F_o|$. [b] $wR_2(F^2) = [\Sigma w(F_o^2 - F_c^2)^2/\Sigma w(F_o^2)^2]^{1/2}$, where $w = 1/[\sigma^2(F_o^2) + (0.1053P)^2 + 10.4315P]$ and $P = (F_o^2 + 2F_c^2)/3$ for **1** and $w = 1/[\sigma^2(F_o^2) + (0.1020P)^2 + 40.2520P]$ and $P = (F_o^2 + 2F_c^2)/3$ for **2**.

Table 2. Selected Bond Distances (Å) and Angles (deg) for **1**[a]

Cu1−N2	2.022(6)	N3−C4	1.494(10)
Cu1−N3	2.004(6)	N3−C5′	1.487(9)
Cu1−O2	2.574(7)	C3−C4	1.508(12)
N1′−C1	1.455(12)	C6″−O1″	1.258(9)
N1′−C2	1.424(11)	C6″−O2	1.245(9)
N2−C2	1.496(10)	C6″−C7″	1.496(10)
N2−C3	1.488(9)	C7″−C8″	1.405(9)
N2−Cu1−N3	86.5(2)	C1−N1′−C2	115.3(8)
N1′−C2−N2	115.0(6)	C2−N2−C3	113.3(6)
N2−C3−C4	108.3(6)	C5′−N3−C4	112.2(6)
N3−C4−C3	108.0(6)	C6″−C7″−C8″	120.5(6)
C3−N2−Cu1	106.3(5)	O1″−C6″−C7″	117.6(7)
C2−N2−Cu1	114.6(5)	O2−C6″−C7″	117.9(7)
C4−N3−Cu1	107.1(4)	O2−C6″−O1″	124.4(7)
C5′−N3−Cu1	115.2(4)		

[a] Symmetry transformations used to generate equivalent atoms: prime, $-x + 1, -y, -z + 1$; double prime, $-y + 1, x - y, z$.

$$BS + G \underset{k_{de}}{\overset{k_{ad}}{\rightleftharpoons}} BS{\cdot}G$$

$$K_f = \frac{k_{ad}}{k_{de}} = \frac{[BS{\cdot}G]}{[BS][G]} \quad (1)$$

If θ is defined as fractional coverage,

$$\theta = \frac{[BS{\cdot}G]}{[BS]_0} = \frac{[G]}{([G] + 1/K_f)}$$

then

$$[BS{\cdot}G]/\omega = \frac{([BS]_0/\omega)[G]}{([G] + 1/K_f)} \quad (2)$$

where ω is amount of host solid/unit volume of the solution (mg/mL).

The plots of the concentration of G bound to BS ([BS·G]) against of [G] were made, and the values of K_f and $[BS]_0/\omega$, the maximum numbers of binding site for guest molecule/g of host solid, were estimated by the analysis of the data according to eq 2.[14]

Results and Discussion

Self-Assembly and X-ray Crystal Structure of 1. By mixing of a DMSO solution of Cu(II) macrocyclic complex of **A** and an aqueous solution of sodium 1,3,5-benzenetricarboxylate (Na_3BTC), 2-D coordination polymer **1** containing 1-D channels was assembled. The solid **1** is insoluble in any solvents except water. It is dissolved in water to dissociate into the building blocks, which was identified by the UV/vis spectrum ($\lambda_{max} = 503$ nm) showing the characteristic chromophore of the starting Cu(II) macrocyclic complex.

Table 3. Selected Bond Distances (Å) and Angles (deg) for **2**

Cu1−N2	2.050(8)	N4−C6	1.44(2)
Cu1−N3	2.008(10)	N4−C7	1.51(2)
Cu1−N5	1.994(10)	N5−C7	1.44(2)
Cu1−N6	2.017(11)	N5−C8	1.50(2)
Cu1−O2	2.415(9)	N6−C9	1.494(14)
Cu1−O4	2.410(8)	N6−C10	1.47(2)
N1−C1	1.51(2)	C11−O1	1.277(14)
N1−C2	1.35(2)	C11−O2	1.256(14)
N1−C10	1.44(2)	C14−O3	1.248(14)
N2−C2	1.56(2)	C14−O4	1.245(13)
N2−C3	1.47(2)	C17−O5	1.223(14)[a]
N3−C4	1.46(2)	C23−O6	1.41(2)[a]
N3−C5	1.494(15)	C29−O7	1.38(2)[a]
N4−C5	1.43(2)		
N2−Cu1−N3	85.5(4)	C14−O4−Cu1	131.1(8)
N2−Cu1−N5	177.9(5)	O1−C11−C12	116.9(10)
N2−Cu1−N6	94.2(4)	O1−C11−O2	126.4(10)
N3−Cu1−N5	93.4(4)	O2−C11−C12	116.7(10)
N3−Cu1−N6	179.4(5)	O2−Cu1−O4	178.3(4)
N5−Cu1−N6	87.0(4)	O3−C14−C15	119.3(9)
N3−Cu1−O2	91.8(3)	O3−C14−O4	122.6(10)
N2−Cu1−O2	94.9(4)	O4−C14−C15	118.1(10)
N2−Cu1−O4	86.6(4)	O5−C17−C18	118.2(19)[a]
N3−Cu1−O4	89.1(3)	O5−C17−C22	122.3(15)[a]
N5−Cu1−O2	86.9(3)	O6−C23−C24	121.5(19)[a]
N5−Cu1−O4	91.7(3)	O6−C23−C28	115.3(18)[a]
N6−Cu1−O2	87.8(3)	O7−C29−C30	118.5(15)[a]
N6−Cu1−O4	91.3(3)	O7−C29−C34	121.8(19)[a]
C11−O2−Cu1	127.2(8)		

[a] For the guest phenol molecules that are not shown in Figure 5a.

The ORTEP drawing of the fundamental building unit of **1** is shown in Figure 1a. The Cu(II) ions show strong tetragonal distortion with average Cu−N(macrocycle) and Cu−O(BTC^{3-}) bond distances of 2.013(3) and 2.574(5) Å, respectively. In the structure of **1**, each Cu(II) macrocyclic complex is coordinated with two BTC^{3-} ions at the apical positions and each BTC^{3-} ion binds three Cu(II) macrocyclic units to generate a 2-D layer extending along the *ab* plane. The coordination polymer layers are not interpenetrated and contain cavities of honeycomb[12] motif, each of which consists of six macrocyclic complexes and six BTC^{3-} ions. The layers pack closely with metal centers and cavities stacked above one another to generate 1-D channels that are perpendicular to the *ab* plane, parallel to the *c* axis. There is no open space on the *bc* or *ac* plane. The distance (Cu···Cu) between two adjacent layers is 6.94 Å, and there exist interlayer interactions: C−H···O hydrogen-bonding interactions, C2···O2 distance = 3.474 Å and C−H−O angle = 136.3°; C−H···π interactions, shortest C···π centroid distance = 4.503 Å.

Within a layer, the diagonal distance (Cu···Cu) of the honeycomb cavity is 17.7 Å and the effective void size is ca. 8.1 Å in diameter (Figure 1b). The BTC^{3-} ions lie alternately above and below the mean 2-D plane, and the thickness of the layer is 7.89 Å including van der Waals

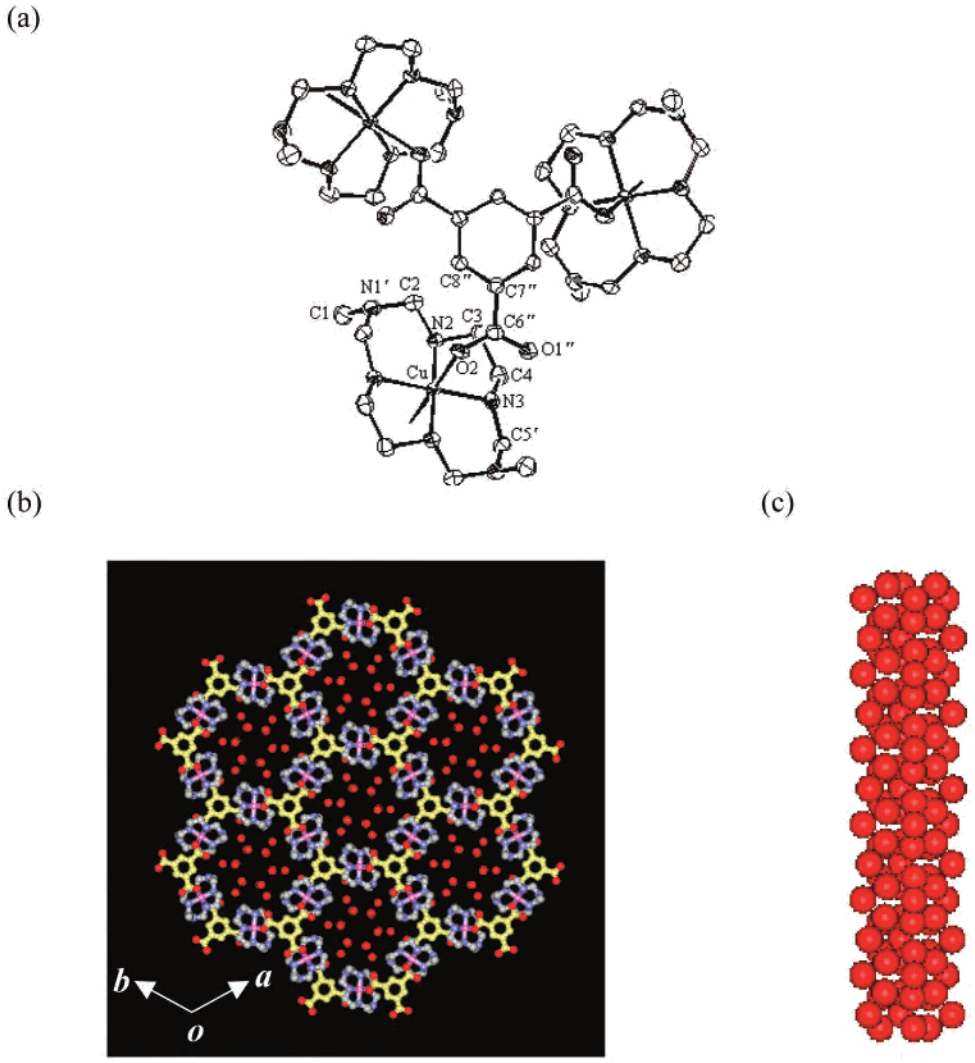

Figure 1. (a) ORTEP drawing of the trinuclear unit of **1** with atomic numbering scheme. The atoms are represented by 30% probable thermal ellipsoids (prime = $-x + 1, -y, -z + 1$ and double prime = $-y + 1, x - y, z$). (b) Packed structure of **1**, showing 1-D channels created perpendicularly to the *ab* plane. (c) Water column created in each channel of **1**. Blue, nitrogen; red, oxygen; orange, copper; gray, carbon of macrocycle; yellow, carbon of BTC^{3-}.

radii of the atoms. The Cu···Cu distance around a BTC^{3-} ion is 8.853(1) Å. The macrocyclic coordination planes are tilted with respect to the benzene ring plane of the coordinating BTC^{3-} ion with the dihedral angles of 41.4°. Three macrocyclic planes linked to a BTC^{3-} have the dihedral angles of 71.4° between them. The 2-D coordination polymeric network is reinforced by the intramolecular hydrogen bonds between the secondary amines of the macrocycle of the Cu(II) complex and the carbonyl oxygen atoms of BTC^{3-} ion (O1···N3, 2.928 Å; N−H−O, 154.8°). The cavities are occupied by water guest molecules, some of which are hydrogen bonded with carbonyl oxygen atoms of BTC^{3-} in the host (O3W···O1, 2.718 Å) and some with other water inclusions (O···O, 2.698−2.879 Å). The void volume in a unit cell is estimated as 566 $Å^3$ (30%) after removing the guest water molecules.[25] The water molecules included in each channel of **1** form a water column along the *c* direction due to the hydrogen-bonding interactions (Figure 1c).

TGA data for the crystalline sample **1** indicate 19.2% loss of weight at 102 °C, indicating that all 18 water guest molecules are removed (see Supporting Information). The remaining compound was heated to 195 °C, without any additional weight loss. At the temperature higher than 195 °C, the compound was decomposed. The crystal morphology of **1** was maintained throughout the heating process up to 170 °C. The XRPD pattern (Figure 2) of the dried solid, which was prepared by heating **1** at 100 °C for 2 h or up to 180 °C at the heating rate of 2.8 °C/min, was coincident with the simulated pattern for the desolvated crystal, indicating that the network structure was unaltered relative to that of **1**.

Guest Exchange Study for 1. When the solid **1** as prepared was immersed in the toluene solutions containing MeOH, EtOH, and PhOH, respectively, some of water molecules in **1** were exchanged with alcohol and phenol but not with toluene. The amount of organic molecules bound to the solid was measured by GC, and the formation constant (K_f) and the numbers of binding site in the host ($[BS]_o$) for guest molecules were estimated according to the methods

(25) Spek, A. L. *PLATON99. A Multipurpose Crystallographic Tool*; Utrecht University: Utrecht, The Netherlands, 1999.

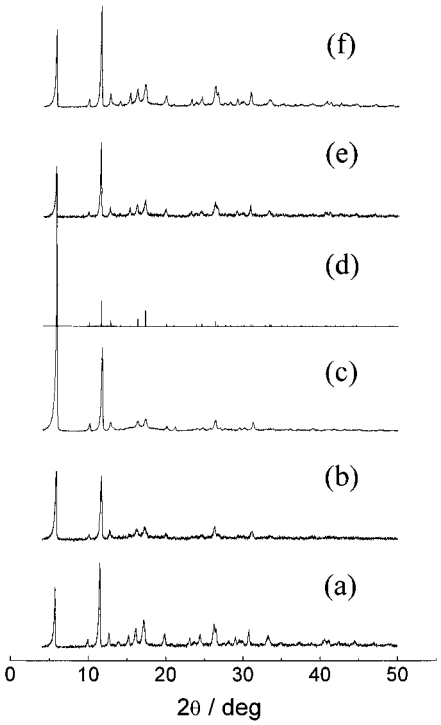

Figure 2. XRPD patterns for (a) original solid **1**, (b) solid **1** dried at 100 °C for 2 h, (c) solid **1** heated at 180 °C with heating speed of 2.8 °C/min, (d) the simulated pattern for the dried solid of **1**, (e) solid obtained by exposing (b) to water vapor for 6 h, and (f) solid obtained by exposing (c) to water vapor for 12 h.

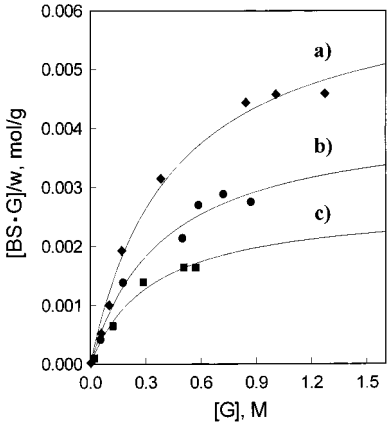

Figure 3. Binding of host solid **1** with organic guests: (a) PhOH (◆); (b) MeOH (●); (c) EtOH (■).

Table 4. Binding Constants of Host Solid **1** with Various Guest Molecules[a]

guest	K_f, M^{-1}	$[BS]_0/\omega$, mmol g^{-1}	guest (mol) included/ unit formula of host solid
PhOH	2.29 ± 0.36	6.48 ± 0.40	10.5
MeOH	2.59 ± 0.90	4.19 ± 0.58	6.78
EtOH	3.02 ± 1.15	2.70 ± 0.46	4.38

[a] Solid **1** as prepared was used.

previously reported.[3,14] The plots of [BS·G] against of [G] are shown in Figure 3, and the values of K_f and $[BS]_0$ are summarized in Table 4. As for the binding constant (K_f), the host solid **1** binds guests in the order EtOH > MeOH > PhOH. However, the values of $[BS]_0/\omega$ indicate that the host solid **1** contains guest-binding sites for 10 PhOH, 7 MeOH, and 4 EtOH mol/formula unit of **1**, which is in volume 1533, 456, and 422 Å^3/unit cell, respectively. The fact that the total volume of PhOH molecules being able to bind **1** is much greater than the void volume (566 Å^3) of **1** suggests that phenol guests must be intercalated between the host layers instead of being included in the channels.

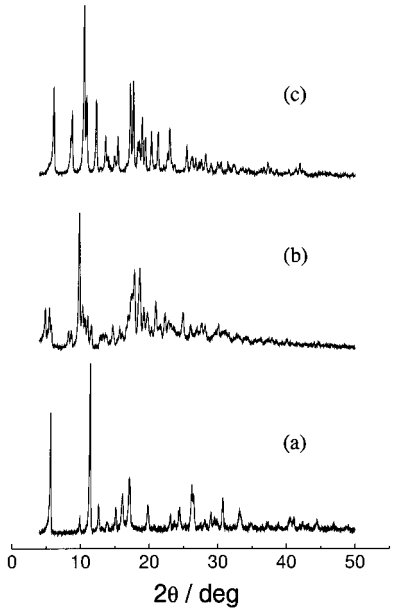

Figure 4. XRPD patterns for (a) **1** as prepared, (b) solid obtained by immersing **1** (0.20 g) in PhOH/toluene (0.80 g/5 mL) for 14 h, and (c) **2** as prepared in water.

Preparation and X-ray Crystal Structure of 2. On the basis of the above result, we tried to isolate the coordination polymer containing phenol guests. By mixing the aqueous solution of **1** with that of phenol, we isolated **2**. In **2**, 9 phenol molecules are included in the unit formula, while the guest binding study in toluene indicated that 10 molecules were included. This difference probably occurs from the experimental error in the guest binding study as well as the different solvent system employed. Figure 4 shows that the XRPD pattern of **2** is different from that of the sample obtained from the binding study in toluene. The solid **2** is insoluble in any solvents except water. It was dissolved in water to dissociate into the building blocks, which was identified by the UV/vis spectrum (λ_{max} = 505 nm) corresponding to the characteristic chromophore of the starting Cu(II) complex. TGA data for the crystalline sample **2** indicate a 4.5% loss of weight at 78 °C, corresponding to the loss of 6 water guest molecules, and additional 37.2% loss of weight at 204 °C, which corresponds to the loss of 9 phenol guests/ formula unit. The crystal morphology of **2** was maintained throughout the heating process up to 160 °C.

The ORTEP drawing of **2** is shown in Figure 5a. The most fascinating observation in **2** is that highly ordered 2-D noncovalent phenol layers are assembled and alternately packed with the Cu(II)−BTC^{3-} coordination polymer layers (Figure 5b−d). The phenol molecules are included in the coordination polymer such that the benzene ring planes lie almost perpendicularly to the coordination polymer layer (Figure 5b,c). The hydroxyl groups of the phenol guests are

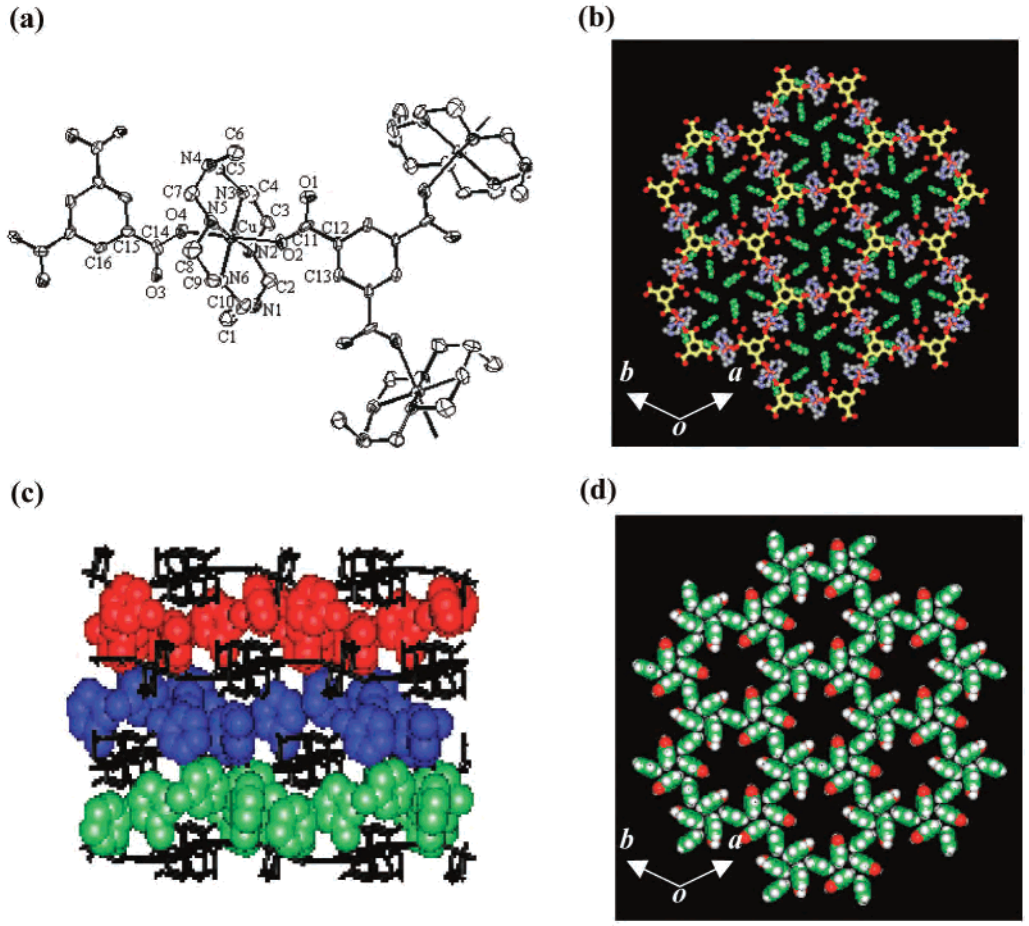

Figure 5. (a) ORTEP drawing of the trinuclear unit of **2** with atomic numbering scheme. The atoms are represented by 40% probable thermal ellipsoids. (b) X-ray structure of **2** (view of the *ab* plane). (c) Side view of **2**. Coordination polymer layers are indicated as black lines, and the noncovalent phenol layers are shown in CPK. (d) View of noncovalent phenol network in **2**. Water inclusions are omitted for clarity. Blue, nitrogen; red, oxygen; orange, copper; gray, carbon of macrocycle; yellow, carbon of BTC^{3-}; green, carbon of phenol.

hydrogen-bonded with the coordination polymer host via uncoordinated carbonyl oxygen atoms of BTC^{3-} (O5···O3, 2.765 Å; O5−H5−O3, 138.4°) and the secondary amines of the macrocycle (O6···N5, 3.124 Å; O6−H5−N5, 132.3°; O7···N2, 3.071 Å; O7−H2−N2, 134.7°). Phenol molecules are linked one another by the edge-to-face $\pi-\pi$ interactions, which generates a highly ordered 2-D noncovalent phenol network (Figure 5d). The centroid separations between the neighboring phenol rings are ca. 5.0 Å, and the ring planes intersect at an angle of ca. 60°. The 2-D phenol network forms honeycomblike cavities, each of which consists of 12 phenol molecules, 6 locating at the corners of the hexagon with ring planes directing toward inside of the cavity and 6 locating on the side of the hexagon by being shared with the adjacent rings. In each cavity, six water guest molecules are included via the hydrogen-bonding interactions with the phenol molecules (O···O, 2.607−2.766 Å; O−H−O, 170−172°).

Compared with the structure of **1**, the structure of the Cu(II)−BTC^{3-} coordination polymer layer in **2** is significantly changed because of the intercalation of the phenol layers. The structures of **1** and **2** are compared in Table 5. The Cu(II) ions show a tetragonal distortion less strong than that in **1**, with average Cu−N(macrocycle) and Cu−O-(BTC^{3-}) bond distances of 2.021(5) and 2.412(6) Å, respectively. The thickness (4.45 Å) of the Cu(II)−BTC^{3-} layer is much smaller than that in **1** because all BTC^{3-} ions locate on the same plane in **2**. The Cu···Cu distances around BTC^{3-} are significantly increased compared with those of **1**; Cu···Cu($-y, x-y, z$) = 10.223(3) Å and Cu···Cu($-y+1, x-y+1, z$) = 10.238(3) Å. The dihedral angle between macrocyclic coordination planes and benzene ring plane of the coordinating BTC^{3-} is on average 75.3°, which is much greater than that (41.4°) of **1**. Three macrocyclic planes linked to a BTC^{3-} ion have a dihedral angle of 68.8° between them. The diagonal distance (Cu···Cu) of the honeycomb ring in the coordination polymer is 20.5 Å, and the effective size of the void is 10.1 Å in diameter, which are increased by ca. 2 Å compared with those of **1**. The shortest Cu···Cu distance between two adjacent layers is 9.985 Å, and the interlayer distance is 8.053 Å, which are also increased as compared with those (8.853 and 6.940 Å) of **1**. In addition to the changes in the thickness of layers, the cavity size of 2-D, and the interlayer distances, the coordination polymer layers of **2** are packed with cavities stacked in the offset

Table 5. Comparison of X-ray Structures of **1** and **2**

host	thickness of layer, Å	interlayer dist, Å	effective void size, Å
1	7.89	6.94	8.1
2	4.45	8.05	10.1

manner, contrary to the structure of **1** (Figure 5c). The density of **2** is reduced from 1.428 g/cm^3 in **1** to 1.280 g/cm^3 due to the intercalation of phenol molecules.

Conclusion

We have assembled a 2-D coordination polymer that generates big 1-D channels perpendicularly to the 2-D layers from the Cu(II) complex of macrocycle **A** and BTC^{3-}. The 2-D open framework binds phenol molecules to generate a highly ordered 2-D noncovalent organic network, which gives rise to a hybrid material combining coordination polymer and noncovalent organic layers. The assembly of highly ordered organic network induced by coordination polymer opens up the possibilities for creation of new materials targeting specific applications, such as aligning organic molecules to generate NLO bulk properties.

Acknowledgment. This work was supported by the Korea Science and Engineering Foundation (Grant 2000-2-12200-002-1) and the Center for Molecular Catalysis.

Supporting Information Available: Figures S1 and S2 for TGA and DTA plots of **1** and **2** and an X-ray crystallographic file for **1** and **2**, in CIF format. This material is available free of charge via the Internet at http://pubs.acs.org.

IC011281U